Available online at www.sciencedirect.com
SCIENCE DIRECT®
Pergamon
Acta Materialia 51 (2003) 1971–1979
Acta MATERIALIA
www.actamat-journals.com

Formation and properties of $Zr_{48}Nb_8Cu_{14}Ni_{12}Be_{18}$ bulk metallic glass

Y. Zhang, D.Q. Zhao, R.J. Wang, W.H. Wang *

Institute of Physics, Chinese Academy of Sciences, P.O. Box 603, Beijing 100080, People's Republic of China

Received 29 November 2001; accepted 23 November 2002

Abstract

$Zr_{48}Nb_8Cu_{14}Ni_{12}Be_{18}$ bulk metallic glass (BMG) with excellent glass-forming ability was prepared by water quenching method. The BMG exhibits high glass transition temperature T_g and onset crystallization temperature T_x, compared with $Zr_{41}Ti_{14}Cu_{12.5}Ni_{10}Be_{22.5}$ BMG. The crystallization processes, change of elastic constants, and density and hardness in the crystallization process were studied by using X-ray diffraction, differential scanning calorimetry and acoustic method. The shear modulus, Poisson ratio, density and hardness are found to be sensitive to the crystallization process. A striking softening of long-wavelength transverse acoustic phonons in the BMG relative to its crystallized state is observed. The linear expansion coefficient, determined by a dilatometer method, is $\alpha_{TG} = 1.04 \times 10^{-5}$ K^{-1} (300–656 K) for the BMG and $\alpha_{TC} = 1.11 \times 10^{-5}$ K^{-1} (356–890 K) for the crystalline alloy. The Mie potential function and the equation of state of the BMG are determined from the expansion coefficient and acoustic experiments.

Keywords: Bulk metallic glass; Properties; Crystallization; Mie potential function

1. Introduction

Since multicomponent bulk metallic glasses (BMGs) especially Zr-based alloys were developed [1-5], the BMGs have attracted increasing interests both in scientific and application aspects. The Zr-based BMGs exhibit unique mechanical properties as well as good wear and corrosion resistance, which could be used in fine optical machinery parts, writing tools, sporting goods and electrodes for generation of chloride gas. $Zr_{65}Al_{7.5}Ni_{10}Cu_{17.5}$ [2], $Zr_{57.5}Al_{7.5}Ni_{10}Cu_{20}Ti_5$ [4], $Zr_{41}Ti_{14}Cu_{12.5}Ni_{10}Be_{22.5}$ [1] and $Zr_{57}Al_{10}Ni_{12.6}Cu_{15.4}Nb_5$ [5] are typical Zr-based BMGs exhibiting excellent glass forming ability (GFA) and high thermal stability, the alloy $Zr_{41}Ti_{14}Cu_{12.5}Ni_{10}Be_{22.5}$ is the best glass former with a critical cooling rate of approximately 1 K/s [3]. It is found that [5,6] the addition or substitution of some elements can significantly improve the formation and properties of the BMG, e.g. the addition of Ti or Nb to the $Zr_{62}Al_{10}Ni_8Cu_{20}$ alloy can distinctly increase glass transition temperature, T_g and onset crystallization temperature T_x [6], tungsten, carbon and carbide addition can improve the thermal stability and mechanical properties of the $Zr_{41}Ti_{14}Cu_{12.5}Ni_{10}Be_{22.5}$ BMG [5]. So a suitable

* Corresponding author. Fax: +86-10-82649531.
E-mail address: whw@aphy.iphy.ac.cn (W.H. Wang).

1359-6454/03/$30.00
doi:10.1016/S1359-6454(02)00602-X

addition and substitution of elements or materials is an effective way to obtain BMG with improving properties.

There has been a long-standing interest in the acoustic, elastic and thermophysical properties of metallic glasses because the studies can provide important information about their structural and vibrational characteristics. The interest is also related to the ever-increasing technological importance of the metallic glasses. However, a comprehensive understanding of the metallic glassy state has been impeded mainly by the inability to prepare bulk specimens before the coming of the BMG. Due to the large size and high thermal stability of the BMG, detailed studies of the thermophysical, acoustic and mechanical properties across a large temperature range become possible. The temperature dependent properties are of particular importance for the BMG, since they can provide a practical method to study the relation between properties and microstructural changes during the relaxation, glass transition and crystallization, and open a way for the understanding of the glassy metallic state.

In this paper, $Zr_{48}Nb_8Cu_{14}Ni_{12}Be_{18}$ BMG was developed by substituting Ti in ZrTiCuNiBe BMG with Nb (Nb has much higher melting temperature), the BMG was found to exhibit excellent GFA and thermal stability [5]. The structural evolution, the changes of elastic constants and thermodynamic parameters of the BMG, such as Young's modulus E, shear modulus G, bulk modulus K, Debye temperature θ_D, and Poison ration μ, upon temperature were determined by X-ray diffraction (XRD) and ultrasonic method. The linear thermal expansion coefficient α_{TG}, upon temperature was measured by the dilatometer method, and the Mie potential function and the equation of the state of the BMG were obtained.

2. Experimental procedure

Ingots with a composition of $Zr_{48}Nb_8Cu_{14}Ni_{12}Be_{18}$ were prepared by arc melting the mixture of the constituent elements in an argon atmosphere. The ingots were remelted in a vacuum-sealed quartz tube and quenched in water. The samples are in shapes of cylindrical rods with diameter of 9 mm and length of 30–80 mm. The details of the preparation procedure can be seen in Ref. [5]. The amorphous nature and homogeneity of the rods were identified by a Siemens D5000 X-ray diffractometry with Cu K_α radiation, differential scanning calorimetry (DSC-7, Perkin Elmer 7). The Vickers hardness was measured by micro-hardness-71 at a load of 200 g.

The metallic glassy rods were machined down to 8 mm in diameter and cut to a length of about 10 mm. By grinding off the outer surface, any possible oxide materials from the quartz tube container were removed, and the identical composition of the three alloys was ascertained by careful chemical analysis. The ends of the cylinder were carefully polished flat and parallel. The prepared specimens were used for density, acoustic velocities and heat measurements. All the measurements were two and three times repeatedly performed using cylinders from different sections of the alloy rods. The acoustic velocities were measured by using a pulse echo overlap method [7]. The excitation and detection of the ultrasonic pulses were provided by X- or Y-cut (for longitudinal and transverse waves, respectively) 10 MHz quartz transducers. The transducers were bonded to one end of the specimen. The ultrasonic waves are excited by the transducer, reflected from the opposite end of the rod, and detected by the same transducer. The effects due to bonding material between the transducer and the samples were neglected as the typical thickness of the band was lower than 4 μm. The travel time of the ultrasonic waves propagating through the sample with a 10 MHz carrying frequency was measured using a MATEC 6600 ultrasonic system with a measuring sensitive of 0.5 ns. Density ρ was measured by the Archimedian principle and the accuracy was evaluated to be 0.005 g/cm^3. The isothermal annealing was performed in a vacuum furnace (10^{-3} Pa), to ensure the same thermal history for all samples each sample was heated up using a rate of 0.17 K/s and cooled with the rate of 0.17 K/s back to room temperature. The thermal expansion was measured by DT-1000 dilatometer produced by the ADAMEL LHOMARGY company of France. The metallic glassy rod was machined down to 2 mm

in diameter and cut to a length of about 13 mm. The specimen was heated at a heating rate of 0.17–893 K, and kept for 300 s, then cooled at 0.17 K/s to the room temperature.

3. Results and discussion

Fig. 1(a) is X-ray diffraction (XRD) pattern of the $Zr_{48}Nb_8Cu_{14}Ni_{12}Be_{18}$ alloy obtained by the water quenching method. The XRD pattern shows a broad diffused peak without any detectable crystallized peaks, indicating an amorphous structure within the examining limit of the XRD. To check the amorphous nature and homogeneity of the rods, the cross-sectional slices cut from a different part of the water quenched rod show the same XRD patterns. The composition of the alloy is confirmed by chemical analysis, the diversity to the nominal composition is within 0.1%. The critical cooling rate for the BMG is estimated to be about 12 K/s [8], indicating that the glass forming system has excellent GFA like the $Zr_{41}Ti_{14}Cu_{12.5}Ni_{10}Be_{22.5}$ BMG. Aluminum is found to be an effective substitution to beryllium in the $Zr_{41}Ti_{14}Cu_{12.5}Ni_{10}Be_{22.5}$ BMG system [2], and $Zr_{57}Cu_{20}$ $Ni_8Al_{10}Ti_5$ [3], $Zr_{57}Cu_{15.4}Ni_{12.6}Al_{10}Nb_5$ [9] are also found to exhibit excellent GFA. In the period table, (Be, Al), (Ti, Nb) are the diagonal elements, they have the similar properties, such as the atomic radius, electronegativity etc., this may be one of reasons for the success of substitution of Al and Nb to Be and Ti in the Zr-based BMG. Fig. 1(b) and (c) are XRD patterns of the $Zr_{48}Nb_8Cu_{14}Ni_{12}Be_{18}$ alloy prepared by the arc melting method (the weight of the ingot is about 24 g) and by water quenching with a slow cooling rate of 4 K/s, respectively. Sharp diffraction peaks can be seen to superimpose on the diffusing amorphous peak. The crystalline peaks are mainly Zr_2Ni Laves's phase.

The DTA curve of the BMG with a heating rate of 0.17 K/s is shown in Fig. 2. Two exothermic peaks followed with an endothermic peak can be seen in the DTA trace. The exothermic peaks are related to the mutlstep crystallization process. Upon further heating, the crystallization sample finally melted at temperature, T_m = 997 K. From the inset DSC trace of the BMG (with a heating rate of 0.17 K/s), a distinct glass transition and a wide supercooled liquid region (SLR) (is referred to as the temperature region between T_x and T_g,

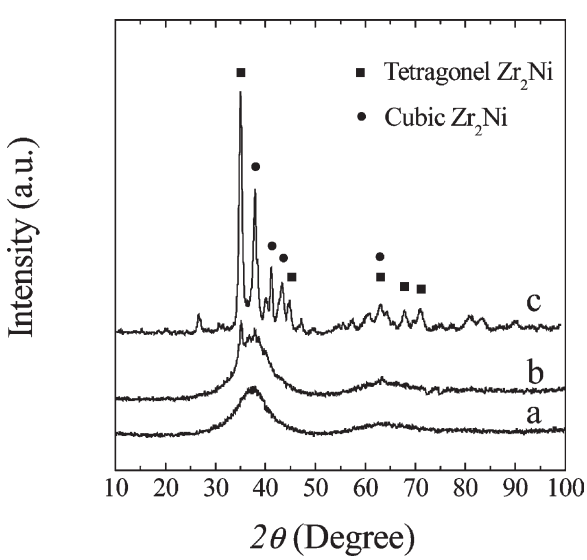

Fig. 1. XRD patterns of $Zr_{48}Nb_8Cu_{14}Ni_{12}Be_{18}$ alloys, (a) water quenched; (b) arc melted ingot (24 g); (c) and slow cooled rod (15 mm in diameter).

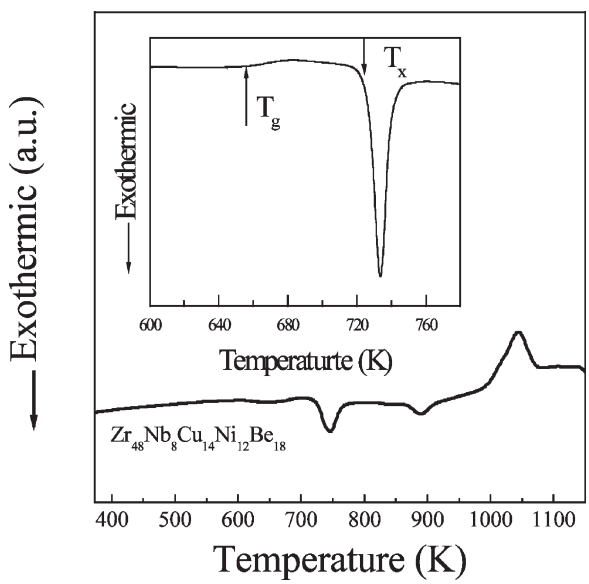

Fig. 2. DTA curve of $Zr_{48}Nb_8Cu_{14}Ni_{12}Be_{18}$ BMG with a heating rate of 0.17 K/s, and the insert is DSC curve with a heating rate of 0.17 K/s between the T_g and T_x.

$\Delta T = T_x - T_g$) can be clearly observed. This is a common feature for almost all the BMGs. For a comparison, the thermal parameters obtained by DSC for $Zr_{41}Ti_{14}Cu_{12.5}Ni_{10}Be_{22.5}$ and $Zr_{48}Nb_8Cu_{14}Ni_{12}Be_{18}$ BMG are listed in Table 1. Both T_g and T_x of the $Zr_{48}Nb_8Cu_{14}Ni_{12}Be_{18}$ BMG have higher values than that of the $Zr_{41}Ti_{14}Cu_{12.5}Ni_{10}Be_{22.5}$ BMG, meaning higher thermal stability. The values of ΔT and reduced glass transition temperature T_{rg} (which is defined as $T_{rg} = T_g/T_m$) of the BMG are 68 K and 0.66, which are close to that of the $Zr_{41}Ti_{14}Cu_{12.5}Ni_{10}Be_{22.5}$ BMG [1]. The values of ΔT and T_{rg} can be used to represent the GFA of a bulk metallic glassy forming system [10]. The above result confirms that the GFA of the $Zr_{48}Nb_8Cu_{14}Ni_{12}Be_{18}$ BMG is almost the same as that of the $Zr_{41}Ti_{14}Cu_{12.5}Ni_{10}Be_{22.5}$ BMG.

The elastic constants can be calculated from the ultrasonic velocities (longitudinal wave velocity v_l and transversal wave velocity v_s) and density ρ [7]. Using the solid theory, the Debye temperature θ_D and specific heat of constant volume C_v can also be determined by [7]:

$$\theta_D = \frac{h}{k}\left(\frac{4\pi}{9}\right)^{-\frac{1}{3}}\rho^{\frac{1}{3}}\left(\frac{1}{v_l^3}+\frac{2}{v_s^3}\right)^{-\frac{1}{3}} \quad (1)$$

$$C_V = 9Nk\left(\frac{T}{\theta_D}\right)^3\int_0^{\frac{\theta_D}{T}}\frac{x^4e^x}{(e^x-1)^2}dx \quad (2)$$

where k is Boltzmann constant, h Planck constant, and N Avogadro's number. The v_l, v_s and ρ of the BMG are 4.95 km/s, 2.26 km/s and 6.70 g/cm^3 respectively. For comparison, the measured and calculated data of the BMG and other Zr-based BMGs are listed in Table 2. The calculated elastic constants from the acoustic velocities are very close to those obtained by other methods [11]. It shows that ρ, microhardness H_V, θ_D and the elastic constants of the BMG are close to that of other Zr-based BMGs. These results indicate that the BMG is of the same excellent properties as that of the other Zr-based BMGs.

To study the relation between the microstructure and properties, the BMG was annealed at different temperatures. The change of the density, elastic constants, hardness, and the structural evolution of the BMG vs temperature were investigated. The XRD patterns in Fig. 3 show the structural evolution of the BMG annealed at different temperatures for 2 h. When the sample is annealed at a low temperature (507 K), no structural change can be observed by XRD, annealing only induces structural relaxation. At 615 K, some crystalline peaks with weak intensity are observed [Fig. 3(b)]. The first precipitation crystalline phase in the amorphous matrix is indexed to be crystalline Zr_2Ni. Long time isothermal annealing below T_g also leads to the precipitation of the nanocrystalline phase. The result is similar to that of the $Zr_{41}Ti_{14}Cu_{12.5}Ni_{10}Be_{22.5}$ BMG [12]. When annealed at 721 K, the BMG is fully crystallized. Beside the main crystalline phase Zr_2Ni, a small amount of crystalline Be_2Zr and other un-identified phases can also be observed [Fig. 3(e)]. The grain size of the crystallite estimated by Scherrer's formula is about 100 nm. In the crystallized ZrTiCuNiBe BMG, however, Ti_2Ni and Zr_2Cu [13] are the main precipitated crystalline phases. Fig. 4(a) presents the changes of G, μ, Hv and ρ with the annealing temperature. It shows that the G and Hv increases slowly with the annealing temperature, and increases drastically near the crystallization temperature. The precipitation at 615 K also causes relatively larger changes of G and Hv, the precipitation enhanced phenomenon has also been observed in ZrTiCuNi BMG [14]. The density also shows a rapid increase near the crystallization temperature. The relative density change between the

Table 1
Thermal properties of $Zr_{48}Nb_8Cu_{14}Ni_{12}Be_{18}$ and $Zr_{41}Ti_{14}Cu_{12.5}Ni_{10}Be_{22.5}$ BMGs determined by DSC at a heating rate of 0.17 K/s

Properties	T_g (K)	T_{x1} (K)	ΔT (K)	T_m (K)	T_g/T_m
$Zr_{48}Nb_8Cu_{14}Ni_{12}Be_{18}$	656	724	68	997	0.66
$Zr_{41}Ti_{14}Cu_{12.5}Ni_{10}Be_{22.5}$	619	690	71	941	0.66

Table 2
The density, hardness and elastic constants calculated from the ultrasonic data for $Zr_{48}Nb_8Cu_{14}Ni_{12}Be_{18}$ and other Zr-based BMGs

Sample	ρ (g/cm^3)	E (GPa)	G (GPa)	K (GPa)	μ	H_V (GPa)	References
$Zr_{48}Nb_8Cu_{14}Ni_{12}Be_{18}$	6.70	93.9	34.3	118.3	0.37	6.09	This work
$Zr_{41}Ti_{14}Cu_{12.5}Ni_{10}Be_{22.5}$	6.13	101.2	37.4	114.1	0.35	5.97	This work
$Zr_{55}Ti_5Cu_{20}Ni_{10}Al_{10}$	6.62	86				5.10	4
$Zr_{57}Nb_5Cu_{15.4}Ni_{12.6}Al_{10}$		84.7	30.8		0.38		8
$Zr_{55}Al_{15}Ni_{10}Cu_{20}$	6.51	90				5.20	4

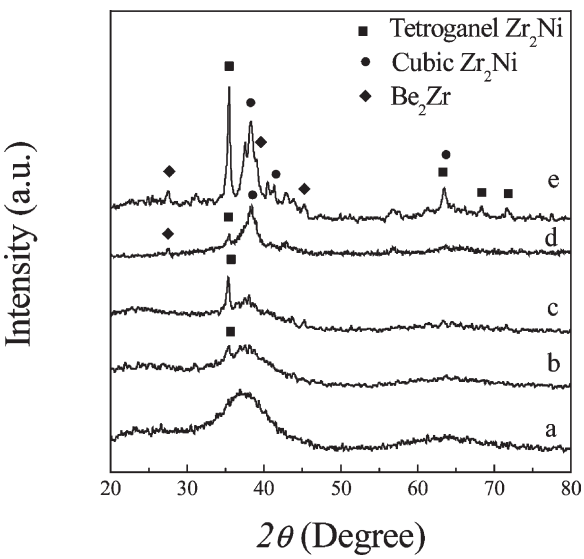

Fig. 3. XRD patterns of $Zr_{48}Nb_8Cu_{14}Ni_{12}Be_{18}$ BMG annealed at different temperatures for 2 h, (a) annealed at 507 K; (b) annealed at 615 K; (c) annealed at 645 K; (d) annealed at 693 K, and (e) annealed at 721 K.

crystallized and as-prepared BMG is about 1.6%, which is larger than that of $Zr_{46.7}Ti_{8.3}Cu_{7.5}Ni_{10}Be_{27.5}$ BMG (0.8%) [15], ZrTiCuNiAl (0.3–0.5%) [4] and the $Zr_{41}Ti_{14}Cu_{12.5}Ni_{10}Be_{22.5}$ BMG [16] (1.2%). The density change between the as-prepared and fully crystallized BMG indicates that an amount of vacancy-like defects or free volume is quenched in the BMG even if it is formed at a low cooling rate. Some of the excess volume is removed during the crystallization. The larger volume change in the Zr-based BMG has also been observed by positron annihilation studies [15] and volume-pressure relation measurements [16]. Table 3 contrasts the large changes in the v_s (8.8%), θ_D (9.5%), and G (20.4%) and small changes in the ρ (1.6%), v_l (4.8%) and K (8.6%) between the as-prepared and fully crystallized BMG. The results indicate the softening of the shear modulus (i.e. the softening of the long wavelength transverse phonons) in the BMG relative to its crystallized state. The softening phenomenon has also been observed during the amorphization process in thin film by irradiation [17–18], and is similar to that associated with melting [17]. The larger softening is not simply attributed to the small density difference between the glassy and crystalline states in the BMG. Lam et al. pointed out that the softening of G is associated with static atomic displacement and anharmonic vibration in an amorphous phase [17]. The effect of the static atomic displacement on the softening was nearly twice as large as that of anharmonic vibration. The static atomic displacement is a general measure of the chemical and topological disorder and hence can be used as a general disorder parameter for characterizing a glass solid [16]. Thus, the structural disorder in the BMG mainly results in the softening of the transverse phonons, which is comparable to that observed for many metals during heating to melting [19]. The softening phenomenon indicates that marked differences exist in the electronic state and atomic interaction between the glassy and crystalline states.

Fig. 5 is the thermal expansion curve with a heating rate of 0.17 K/s. It shows that the relative length of the alloy in a glassy state increases linearly with increasing temperature. As the temperature reaches T_g temperature (656 K), the length begins to decrease slowly, when the temperature reaches T_x (724 K), the length changes drastically. However, when the crystallized alloy is cooled with a heating rate of 0.17 K/s, no drastic length

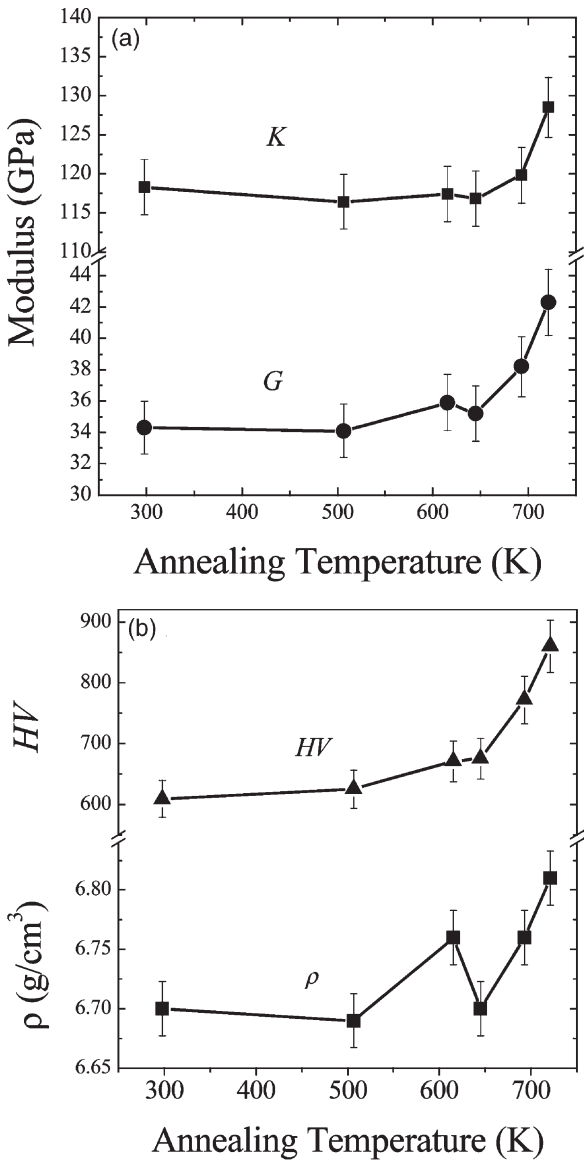

Fig. 4. Shear and bulk moduli (G and K) change of $Zr_{48}Nb_8Cu_{14}Ni_{12}Be_{18}$ BMG upon annealing temperatures (a), and the hardness and density change of $Zr_{48}Nb_8Cu_{14}Ni_{12}Be_{18}$ BMG upon the annealing temperatures (b).

change is observed. Similar thermal expansion phenomenon has also been observed in other BMGs [20]. By fitting the curve, we obtained the linear thermal expansion coefficients of $\alpha_{TG} = 1.04 \times 10^{-5}$ K^{-1} (300–656 K) for the BMG and $\alpha_{TC} = 1.11 \times 10^{-5}$ K^{-1} (356–890 K) for the crystallized state. The measured linear thermal expansion coefficients are in accord with those of the reported result for the other Zr-based BMGs [20–21]. The crystallization volume fraction of the BMG during the crystallization process vs temperature can be estimated by the relative length change between T_g and T_x of the specimen. The transformation ratio starts to increase near the T_g and increases quickly near the T_x as shown in Fig. 6.

The well known Grueneisen equation of a solid can be expressed as follows [22]:

$$\gamma = \frac{3\alpha_T K_0 V_0}{C_V} = \frac{n+2}{6} \tag{3}$$

where α_T is the linear thermal expansion coefficient, γ Gruneisen constant, and C_V the specific heat at constant volume, and K_0 and V_0 are the bulk modulus and atomic volume at $T = 0$ K and pressure $P = 0$ Pa, respectively. n is the parameter in the Mie potential:

$$\varphi = -\frac{A}{V^{m/3}} + \frac{B}{V^{n/3}}, \tag{4}$$

where V is the atomic volume, A and B are constants with positive values, m is the exponent for the attractive part. In general, $m = 3$ for metal, n is the exponent of the repulsive part and its value varies in a large range depending on the materials. From the first rule of Grueneisen, the sublimation, φ_0 is [22]:

$$-\varphi_0 = \frac{9}{mn} V_0 K_0. \tag{5}$$

At $T = 0$ K and $P = 0$ Pa,

$$P = -\left.\frac{d\varphi}{dV}\right|_{V=V_0} = -\frac{\frac{m}{3}A}{V_0^{\frac{m}{3}+1}} + \frac{\frac{n}{3}B}{V_0^{\frac{n}{3}+1}} = 0 \tag{6}$$

and K is defined as:

$$K = -V\frac{dP}{dV} = V\left.\frac{d^2\varphi}{dV^2}\right|_{V=V_0} = K_0 \tag{7}$$

let $V_0 \approx V$ ($T = 273$ K) = 10.266 cm^3/mol, and $K_0 \approx K$ ($T = 273$ K) = 118.3 GPa. The value of ϕ_0

Table 3
A comparison of properties of amorphous state (Y_a) and crystallized state (Y_c) of the $Zr_{48}Nb_8Cu_{14}Ni_{12}Be_{18}$ BMG

State	ρ (g/cm^3)	V_l (m/s)	V_s (m/s)	G (GPa)	K (GPa)	θ_D (K)
Amorphous	6.70	4.95	2.26	34.3	118.3	295
Crystallized	6.81	5.19	2.46	41.3	128.5	323
$(Y_c-Y_a)/Y_a$	1.6%	4.8%	8.8%	20.4%	8.6%	9.5%

Table 4
The calculated value of m, n, γ, A and B of the Mie potential for the metallic glassy and crystallized states of the $Zr_{48}Nb_8Cu_{14}Ni_{12}Be_{18}$ alloy

Parameters	Glassy state	Crystallized state
α	1.04×10^{-5} K^{-1}	1.11×10^{-5} K^{-1}
K	118.3 GPa	128.5 GPa
C_V	23.7 J(mol K)$^{-1}$	23.5 J(mol K)$^{-1}$
V_0	10.266 Cm^3/mol	10.100 Cm^3/mol
ϕ_0	503 KJ/mol	508 KJ/mol
γ	1.59	1.84
n	7.54	9.04
m	2.88	2.54
A	13.40	41.68
B	8.44×10^{-8}	1.66×10^{-10}

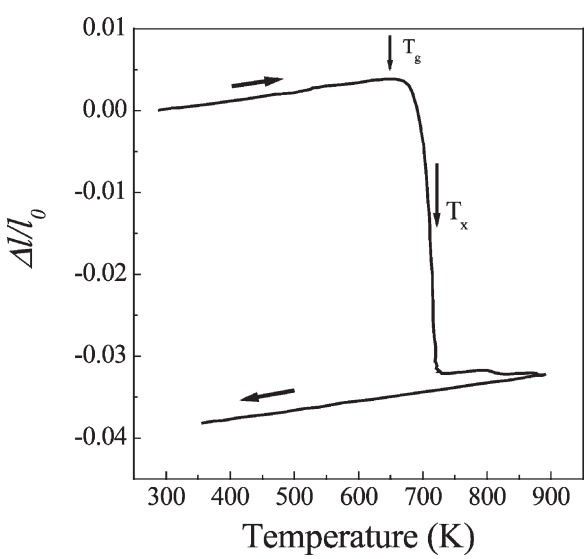

Fig. 5. Relative length ($\Delta l/l_0$) change of $Zr_{48}Nb_8Cu_{14}Ni_{12}Be_{18}$ BMG upon temperature, both the heating and cooling rate are 0.17 K/s. l_0 is the length of the sample at room temperature.

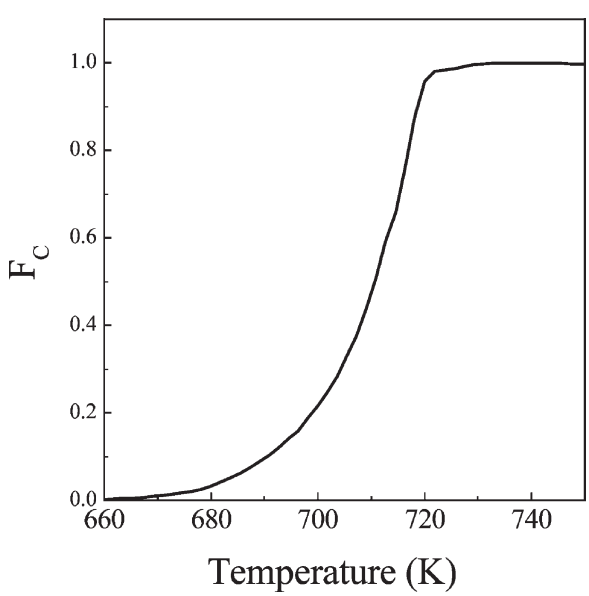

Fig. 6. Change in the ratio of crystalline fraction transformation (F_C) calculated from the length change with the heating temperature. The heating rate is 0.17 K/s.

of the crystallized alloy can be estimated by using the sublimation data of pure components of the alloy [23–24]. These components are postulated in ideal mixing, and ϕ_0 of the crystallized state is the sum of the ϕ_0 of the glassy state and crystallization enthalpy. The values of Cv, θ_D and K are obtained from the acoustic data and listed in Table 1. From Eqs. (3)–(7), the values of m, n, γ, A and B for the glassy and crystallized states can be estimated, and the results are listed in Table 4. Thus, the Mie potential and the P–V relation at $T = 0$ K for the $Zr_{48}Nb_8Cu_{14}Ni_{12}Be_{18}$ BMG are described respectively as:

$$\varphi = -\frac{13.40}{V^{0.96}} + \frac{8.44 \times 10^{-8}}{V^{2.513}} \tag{8}$$

$$P(V,0) = -\frac{7.28 \times 10^3}{V^{1.96}} + \frac{2.71 \times 10^5}{V^{3.513}} \text{ (GPa)}. \tag{9}$$

For the crystallized state, the Mie potential and the P–V relation at $T = 0$ K are:

$$\varphi = -\frac{41.68}{V^{0.85}} + \frac{1.66 \times 10^{-10}}{V^{3.013}} \tag{10}$$

$$P(V,0) = -\frac{4.27 \times 10^3}{V^{1.85}} + \frac{6.35 \times 10^5}{V^{4.013}} \text{ (GPa)}. \tag{11}$$

For the equation of state of the alloy at elevated temperatures, it is related to the pressure at absolute zero $P(V,0)$ and the thermal pressure $P_D(V,T)$ (the electron thermal contribution can be neglected when $T < 10^4$ K):

$$P(V,T) = P(V,0) + P_D(V,T). \tag{12}$$

The term for the thermal pressure due to lattice vibrations is estimated from the expression [25]

$$P_D(V,T) = \frac{3Nk_BT\gamma(V)}{V} D\left(\frac{\theta_D}{T}\right) \tag{13}$$

where N is Avogadro constant, k_B is Boltzmann constant, $\gamma(V)$ is the Grueneisen coefficient, θ_D is Debye temperature, $D\left(\frac{\theta_D}{T}\right) = \frac{3}{x^3}\int_0^x \frac{\xi^3 d\xi}{e^\xi - 1}, x = \frac{\theta_D}{T}$. In our case ($P < 15$ GPa), $\gamma(V) \approx \gamma$. Thus from Eqs. (8)–(13) the EOS of the BMG and its corresponding crystallized state can be expressed as follows:

$$P(V,T) = -\frac{7.28 \times 10^3}{V^{1.96}} + \frac{2.71 \times 10^5}{V^{3.513}} + \frac{39.64T}{V} D\left(\frac{\theta_D}{T}\right) \tag{14}$$

for the BMG

$$P(V,0) = -\frac{4.27 \times 10^3}{V^{1.85}} + \frac{6.35 \times 10^5}{V^{4.013}} + \frac{45.87T}{V} D\left(\frac{\theta_D}{T}\right) \tag{15}$$

for the crystallized alloy.

The value of $D\left(\frac{\theta_D}{T}\right)$ can be obtained at any given temperature from a table in Ref. [25]. Thus, it is possible to determine the magnitude of the thermal pressure at any given temperature. For high temperature, $x \ll 1$,

$$P_D(V,T) = \frac{3Nk_BT\gamma}{V} \tag{16}$$

For low temperature, $x \gg 1$,

$$P_D(V,T) = \frac{3}{5}\pi^4 \left(\frac{T}{\theta_D}\right)^3 \frac{Nk_BT\gamma}{V}. \tag{17}$$

Fig. 7 presents the P–V relation for both of the metallic glassy and crystallized states of the $Zr_{48}Nb_8Cu_{14}Ni_{12}Be_{18}$ alloy at room temperature. The obtained equation of state is close to that of $Zr_{41}Ti_{14}Cu_{12.5}Ni_{10}Be_{22.5}$ BMG obtained by direct P–V measurements at room temperature [16].

4. Conclusions

The $Zr_{48}Nb_8Cu_{14}Ni_{12}Be_{18}$ BMG with excellent glass forming ability and high thermal stability was obtained. The BMG is found to have the same

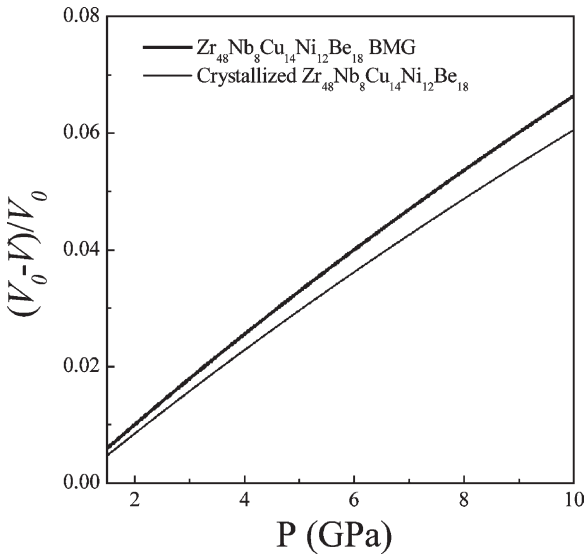

Fig. 7. The *P–V* relation of the $Zr_{48}Nb_8Cu_{14}Ni_{12}Be_{18}$ alloy in glassy and crystalline states.

excellent properties as that of the other Zr-based BMGs. The density change between the as-prepared and fully crystallized BMG indicates that an amount of vacancy-like defects or free volume is quenched in the BMG even if it is formed at low cooling rate. A striking softening of long-wavelength transverse acoustic phonons in the BMG relative to its crystallized state is observed. The linear expansion coefficient, determined by a dilatometer method, is $\alpha_{TG} = 1.04 \times 10^{-5}$ K^{-1} (300–656 K) for the BMG and $\alpha_{TC} = 1.11 \times 10^{-5}$ K^{-1} (356–890 K) for the crystalline alloy. The Mie potential and the equation of state of the BMG are obtained from the expansion coefficient experiments.

Acknowledgements

The authors are grateful for the financial support of the National Natural Science Foundation of China (Granted numbers: 59925101 and 50031010) and National Microgravity laboratory of CAS. The valuable discussion with Dr. M.X. Pan is greatly appreciated.

References

[1] Peker A, Johnson WL. Appl Phys Lett 1994;63:2342.
[2] Inoue A, Zhang T, Masumoto T. Mater Trans, JIM 1990;31:177.
[3] Xing LQ, Eckert J, Loser W, Schultz L. Appl Phys Lett 1999;74:664.
[4] Zhang T, Inoue A. Mater Trans, JIM 1998;39:1230.
[5] Zhang Y, Zhao DQ, Wang RJ, Pan MX, Wang WH. Mater Trans, JIM 2000;41:1423.
[6] Choi H, Johnson WL, Appl Phys Lett, 71, (1997) 3808; Kato H, Inoue A, Mater Trans JIM, 38, (1997) 793.
[7] Schreiber D. Elastic constants and their measurements. New York: McGraw-Hill, 1973. In: Kittel C, Introduction to solid state physics. John Wiley and Sons, 1991.
[8] Lin XH, Johnson WL. J Appl Phys 1995;78:6514.
[9] Conner RD, Choi-Yim H, Johnson WL. J Mater Res 1999;14:3292.
[10] Inoue A, Zhang T, Takeuchi A. Mater Sci Forum 1998;269-272:855.
[11] Wang WH, Wang RJ, Li FY, Zhao DQ, Pan MX, Appl. Phys. Lett., 74, 1803 (1999); Conner RD, Dandliker RB, Johnson WL, Acta Mater., 46, 6089 (1998).
[12] Schneider S, Thiyagarajam P, Johnson WL. Appl Phys Lett 1996;68:493.
[13] Hays CC, Kim CP, Johnson WL. Appl Phys Lett 1999;75:1089.
[14] Frankwicz PS, Ram S, Fecht H-J. Appl Phys Lett 1996;68:2825.
[15] Nagel C, Ratzke K, Schmidtke E, Wolff J, Geyer U, Faupel F. Phys Rev B 1998;57(4):10224.
[16] Wang WH, Bao ZX, Liu CX, Zhao DQ, Eckert J. Phys Rev B 2000;61:3166.
[17] Lam NQ, Okamoto PR. MRS Bulletin 1994;19:41.
[18] Zuk J, Kiefer H, Clouter MJ. Appl J Phys 1993;73:4851.
[19] Testardi LR, Krause JT, Chen HS. Phys Rev B 1973;8:4464.
[20] Ohsaka K, Chung SK, Rhim WK, Peker A, Scruggs D, Johnson WL. Appl Phys Lett 1997;70:726.
[21] Damaschke B, Samwer K. Appl Phys Lett 1999;75:2220.
[22] Gruneisen E. Handbuch der Physik 1926;10:1–52.
[23] Davies HA. Phys Chem Glasses 1976;17:159.
[24] Kubaschewski O, Alcock CB, Spencer PJ. Material thermochemistry, 6th ed. Pergamon Press, 1993 p. 322.
[25] Bradley RS. High pressure physics & chemistry. London: Academic Press, 1963.